A Numerical Simulation of "5.5" Super-Duststorm in Northern China

Li Xingsheng (李兴生), *Zhou Jianqiang* (周建强), *Li Zhe*[1], *Fang Xiumei* (房秀梅) and *He Zhuanshi* (何颛士), *Farn Parungo*[2]

Chinese Academy of Meteorological Sciences, Beijing 100081

Received February 24, 1997; revised May 12, 1997

ABSTRACT

Combining the Penn State / NCAR mesoscale (MM4) model, the dust transport model and an atmospheric radiative transfer model, a super duststorm process occurred in the Gansu province on 5 May 1993 has been simulated. Based on the observations of duststorms occurred in the northern China and the field measurements of dust particles' physical and optical properties, model simulating dust plume transport processes and dust particle radiative forcing have been devloped. The models are described and verified with real cases of duststorms.

Key words: Duststorm, Physical process, Radiative forcing

I. INTRODUCTION

In the past a few decades, the mechanism of the duststorm has been studied in terms of numerical simulations. A two-dimensional steady duststorm transport model was established by Schutz (1980), in which the turbulence diffusion, gravity deposition and long distance transport processes are involved, the model was used to study duststorm transport over the Atlantic Equator area. Obviously, the steady model was only with the simple source and the transport process. Berkofsky (1982) developed a one-dimensional model with vertical advection, turbulence diffusion and gravity deposition, to study the temporal and spectral variation of the dust aerosols, and the sands of uniform size and shape with height were assumed. Lee (1983) used a three-dimensional mixing layer model to calculate the variations of the concentration of Saharan duststorm in long-range transport, besides the same physical processes mentioned above, the condensation effect of the dust particles was included. Despite this model had made much improvement than before, but only one level was in this model as a mixing layer (or atmospheric boundary layer), that means the dust particles in the mixing-layer spread immediately in spite of the dust sizes. Undoubtedly, the deposition time for large particles will be extended. Westpal (1987) developed a two-dimensional transport model, combining NCAR dynamic model and NASA aerosols transport model into one. Many main characters of the dust in the atmospheric boundary layer were simulated.

On 4-7 May 1993, a strong cold wind storm passed through the northwestern China as shown in Figure 1a, which generated a super duststorm in many provinces, including Xinjiang, Gansu, Ningxia. In Jinchang city, the 10 min average wind speed was 22.0 m / s—25.3 m / s, with a maximum of 34 m / s. During the passage of the duststorm (Fig. 1b), visibility reduced to zero and the concentrations of airborne dust was >1 g / m^3. After the duststorm the temperature decreased to -2°C—2°C in many areas generally.

[1] University of Colorado at Boulder, CO 80309, U. S. A.

[2] Science and Technology Corporation, Boulder, CO 80303, U. S. A.

The surface weather map at 0800 local time (LT) on 5 May indicated a high pressure center in the northwest of Xinjiang approaching 1034 hPa; the air pressure at Hexi Corridor was low; and the pressure difference between both locations reached 30 hPa. At 1400 LT, the 3 hours pressure difference around the cold front was 9 hPa, at 1700 LT that became 13 hPa. The strong pressure gradient had potential for the formation of strong flow. The cold front arrived to the central Hexi Corridor at noon, the surface temperature of Zhangye ahead of the cold front was 25°C, but at Dingxing behind the cold front it was 7°C; thus the temperature difference within one longitude reached 18°C. The average moving speed of the cold front was indicated at 50–60 km / hr. The entire range of dynamic and thermal conditions played an important role in this super duststorm.

II. MODEL DESCRIPTION

2.1 *MM4 Governing Equations*

The Penn State / NCAR Mesoscale Model (MM4) based on the original version described by Anthes and Warner (1978) is adopted. The vertical σ–coordinate is defined in terms of pressure,

$$\sigma = \frac{p - p_t}{p_s - p_t} \quad , \tag{1}$$

where p_s and p_t are the surface and top pressure of the model, respectively; p_t is a constant. The model equations are given, where $p^* = p_s - p_t$.

$$\frac{\partial p^* u}{\partial t} = -m^2 \left(\frac{\frac{\partial p^* uu}{m}}{\partial x} + \frac{\frac{\partial p^* uv}{m}}{\partial y}\right) - \frac{\partial p^* u\dot{\sigma}}{\partial \sigma} - mp^* \left(\frac{RT_v}{p^* + \frac{p_t}{\sigma}} \frac{\partial p^*}{\partial x} + \frac{\partial \Phi}{\partial x}\right) + fp^* v + \left.\frac{\partial p^* u}{\partial t}\right|_{\text{CUB}} + \left.\frac{\partial p^* u}{\partial t}\right|_{\text{PBL}} + \left.\frac{\partial p^* u}{\partial t}\right|_{\text{DIFF}} \quad , \tag{2}$$

$$\frac{\partial p^* v}{\partial t} = -m^2 \left(\frac{\frac{\partial p^* uv}{m}}{\partial x} + \frac{\frac{\partial p^* vv}{m}}{\partial y}\right) - \frac{\partial p^* v\dot{\sigma}}{\partial \sigma} - mp^* \left(\frac{RT_v}{p^* + \frac{p_t}{\sigma}} \frac{\partial p^*}{\partial y} + \frac{\partial \Phi}{\partial y}\right) - fp^* u + \left.\frac{\partial p^* v}{\partial t}\right|_{\text{CUB}} + \left.\frac{\partial p^* v}{\partial t}\right|_{\text{PBL}} + \left.\frac{\partial p^* v}{\partial t}\right|_{\text{DIFF}} \quad , \tag{3}$$

$$\frac{\partial p^*}{\partial t} = -m^2 \left(\frac{\frac{\partial p^* u}{m}}{\partial x} + \frac{\frac{\partial p^* v}{m}}{\partial y}\right) - \frac{\partial p^* \dot{\sigma}}{\partial \sigma} \quad , \tag{4}$$

$$\dot{\sigma} = -\frac{1}{p^*} \int_0^\sigma \left[\frac{\partial p^*}{\partial t} + m^2 \left(\frac{\frac{\partial p^* u}{m}}{\partial x} + \frac{\frac{\partial p^* v}{m}}{\partial y}\right)\right] d\sigma \quad , \tag{5}$$

$$\frac{\partial p^* T}{\partial t} = -m^2\left(\frac{\frac{\partial p^* uT}{\partial x}}{m} + \frac{\frac{\partial p^* vT}{\partial y}}{m}\right) - \frac{\partial p^* T\dot{\sigma}}{\partial \sigma} - \frac{RT_v\omega}{C_{pm}(\sigma + \frac{p_t}{p^*})} + \frac{p^* Q}{C_{pm}}$$

$$+ \left.\frac{\partial p^* T}{\partial t}\right|_{\mathrm{CUB}} + \left.\frac{\partial p^* T}{\partial t}\right|_{\mathrm{PBL}} + \left.\frac{\partial p^* T}{\partial t}\right|_{\mathrm{DIFF}} , \tag{6}$$

$$\omega = p^* \dot{\sigma} + \frac{\sigma dp^*}{dt} , \tag{7}$$

$$\frac{dp^*}{dt} = \frac{\partial p^*}{\partial t} + m\left(u\frac{\partial p^*}{\partial x} + v\frac{\partial p^*}{\partial y}\right) , \tag{8}$$

$$\frac{\partial \Phi}{\partial \ln(\sigma + \frac{p_t}{p^*})} = -RT_v\left(1 + \frac{q_c + q_r}{1 + q_v}\right)^{-1} , \tag{9}$$

where u and v are components of wind velocity in eastward amd northward direction; T and q are temperature and mixing ratio of water vapor, respectively; Φ is the geopotential height; C_p is the specific heat at constant pressure; R is the universal gas constant; m is the map scale factor; Q is the heating rate; CUB represents time variation caused by cumulus convective motion; DIFF represents subgrid horizontal diffusion.

2.2. *Dust Particle Transport Equation*

The same description is given for the dust aerosols transport equation as for the MM4 model equations:

$$\frac{p^* C(r)}{\partial t} = -m^2\left(\frac{\frac{\partial p^* uC(r)}{\partial x}}{m} + \frac{\frac{\partial p^* vC(r)}{\partial y}}{m}\right) - \frac{\partial p^* C(r)\dot{\sigma}}{\partial \sigma}$$

$$+ \left.\frac{\partial p^* C(r)}{\partial t}\right|_{\mathrm{drop}} + \left.\frac{\partial p^* C(r)}{\partial t}\right|_{\mathrm{PBL}} + \left.\frac{\partial p^* C(r)}{\partial t}\right|_{\mathrm{DIFF}} + \left.\frac{\partial p^* C(r)}{\partial t}\right|_{\mathrm{S}} , \tag{10}$$

where r is the radius of the dust aerosol particles; $C(r)$ is the aerosol concentration with r radius;DROP represents the variation of dust aerosols concenttration caused by deposition;

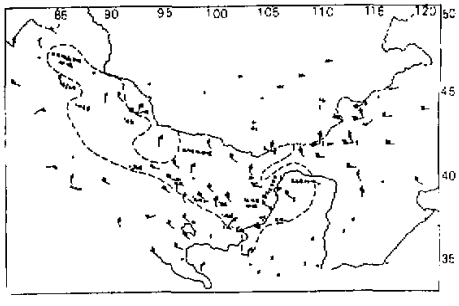

Fig.1a. Weather map for 4–7 May 1993. A super duststorm passed through the northwestern China within the dash-line region.

Figure 1b. Photograph of duststorm approaching Jin'chang City.

DIFF represents the horizontal diffusion of the dust aerosols concentration; and S represents the effect of variation of the dust source.

2.2.1 *Dust size distributions*

For parameter of the dust particle size distributions, the volume ratio of the neighboring particle sizes is assumed to be a constant.

$$\text{constant} = \frac{V_{i+1}}{V_i} \quad , \tag{11}$$

where V_i and V_{i+1} are the volumes of the dust particles of ith and $i+1$th, respectively. If the forms of the dust particles are spheres, then the equation can be rewritten as

$$\text{constant} = \left(\frac{r_{i+1}}{r_i}\right)^3 \quad . \tag{12}$$

Taking const = 4, the dust particles are divided into 13 classes shown in Table 1, the minimum size radius is 0.25 μm and the maximum size radius is 64.0 μm.

Table 1. The Distribution of the Dust Particles Radii (μm)

class	1	2	3	4	5	6	7	8	9	10	11	12	13
radius (r_i)	0.25	0.40	0.63	1.00	1.59	2.52	4.00	6.35	10.1	16.0	25.4	40.3	64.0

2.2.2 *Dust sources*

For the parameter of the dust sources, which play an important role in duststorm development strength, as well as size distributions of dust particles, the model simulates them as items of surface friction velocity u_*. The lifting of the dust particles from the surface requires a force surpassing a critical surface wind velocity. A team monitored the Chinese deserts and the Loess Plateau reported that the critical surface wind velocity varied from 6 m/s to 8 m/s, depending on surface characteristics. However the critical friction velocity was not measured. Westphal et al. (1987) obtained an average critical friction velocity in Saharan duststorms to be 45 cm/s. Gillette et al. (1981) found that the dust particles flux approaches to zero as the surface friction velocity decreases below a critical value. In this model simulation the critical friction velocity is chosen as 50 cm/s.

On the basis of the results assumed by Westphal et al. (1987), the dust flux of the particle size spectra can be defined as

$$F_a = 1.6 \times 10^{-13} u_*^4 \quad , \tag{13}$$

then the source strength can be written as

$$S = \frac{F_a}{\Delta Z} = 1.6 \times 10^{-13} \frac{u_*^4}{\Delta Z} \quad . \tag{14}$$

If the source strength of each range particle size is $s(r)$, which can be taken as

$$S(r) = S \times f(r) \quad , \tag{15}$$

where $f(r)$ is a distribution factor being of a relationship with the dust flux as

$$f(r)=\frac{r^{1.5}}{\sum r_i^{1.5}} \quad . \tag{16}$$

Finally, we have

$$\left.\frac{\partial p^* C(r)}{\partial t}\right|_s = p^* S(r)=\frac{1.6\times 10^{-13}u_*^4}{\Delta Z}\frac{r^{1.5}}{\sum r_i^{1.5}}p^* \quad . \tag{17}$$

2.2.3 *Dust dry deposition parameterization*

For parameterization of dust dry deposition, only gravity and turbulence effects are considered in this model simulation. According to the Stokes equation and as all dust particles are assumed to be spheres, the gravity deposition veolocity will be

$$V_g(r)=\frac{2}{9}\frac{\rho-\rho_a}{\eta}gr^2 \quad , \tag{18}$$

where ρ and ρ_a are densities of the dust particle and the air, respectively; η is the air viscosity coefficient. Because the air density is much less than the density of dust particles, the equation for the gravity deposition velocity can be changed as

$$V_g(r)\approx\frac{2}{9}\frac{\rho g r^2}{\eta} \quad . \tag{19}$$

Finally, the dry deposition term in the dust transport equation will be

$$\left.\frac{\partial p^* C(r)}{\partial t}\right|_{\text{drop}} = -\frac{\partial(\rho g V_g(r)C(r))}{\partial\sigma} = -\rho g V_g(r)\frac{\Delta C(r)}{\Delta\sigma} \quad . \tag{20}$$

2.2.4 *Atmospheric radiation parameterization*

For the parameterization of atmospheric radiation, the dust indirect effect on radiation via cloud process is ignored because the air is usually dry and the cloud cover is generally low during a duststorm. The main factor affecting the atmospheric radiation is extinction by the dust particles. The contributing factors are absorption and scattering of the water vapor, ozone and carbon-dioxide.

Although variabilities are known on dust composition, concentration, and size distribution during the dust plume transport, for simplicity, an average status of the aerosols in a duststorm is taken into account in terms of a standard radiation atmospheric (SRA) mode. In this model simulation the SRA mode, suggested by the radiation council of the International Association of Meteorology and Atmospheric Sciences (IAMAP), was used for calculating the atmospheric radiation transmission and heat budget. By using the logarithm normal and the collective distributions, the spectrum of atmospheric aerosols can be expressed as:

$$\frac{dN(r)}{d(\ln r)}=\frac{N}{\sqrt{2\pi}}\exp\left[\frac{(\ln r-\ln R)^2}{2(\ln\delta)^2}\right] \tag{21}$$

and

$$\frac{dN(r)}{dr}=Ar[\exp(-br^t)] \quad . \tag{22}$$

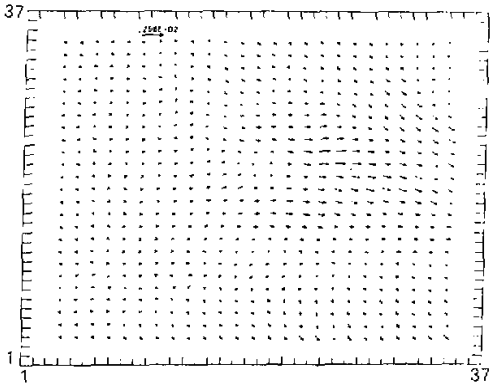

Fig.2. The horizontal wind speed field of 500 hPa on 5 May 1993 at 1400 BJT.

III. SIMULATED RESULTS

The simulated area chosen is 30°N— 55°N and 70°E— 120°E; the center is 95.5°E, 45.5°N. The nested simulation area is 35°N—45°N and 95°E—110°E; the center is 102°E, 39.4°N. Both horizontal grid points are 37 × 37; the simulation area grid size is 90 km and the nested simulation grid size is 30 km. The vertical direction is divided into 15 levels. The initial integrating time is from 00 hr (GMT) 4 May 1993; the time-step is 3 min, and the total integrating time is 36 hr.

In order to understand the duststorm transport process and the effect of the dust particles on radiation, two simulated cases are designed. In case A, without radiation effect, the dust sources are around the Zhungeer Basin and Hexi Corridor; In case B, the simulated conditions are the same as the case A, but the effect of the dust particles on radiation is included.

3.1 *Case A*

3.1.1 *Meteorological field*

On 5 May 1993 at 0800 BJT was simulated as a trough on 500 hPa and developed with a center at 95.5°E and 55.5°N. The temperature distribution, which corresponds to potential height field, formed a low-temperature / low-pressure system. At 1400 BJT a high-level jet zonal on 500 hPa was located at the desert area, posing potential for a strong duststorm at Hexi Corridor. As shown in Fig 2, the simulated results of nest-grid indicated that the narrow Hexi Corridor topographic effect also contributed to the strong flow, which indicate the duststorm transport.

The nest-grid map of 700 hPa on 5 May at 1400 BJT indicates a typical meso-scale weather process, a warm ridge at 100°E, 40°N from the Tibet an Plateau extending to north, as shown in Fig 3, and next to that a cold trough extending to southwest (dark dotted line in Fig 3). The simulated area approaching Jinchang City was controlled by a low pressure center, its scale was about 500 km × 400 km, that associated with the temperature distribution causing steeper temperature gradients, as shown in Fig 4. The distributions of the vertical velocity and horizontal velocity on 700 hPa around Jinchang City consist of a strong upward (Fig 5) and a strong convergence area (Fig 6). As a result, a super-severe duststorm with low

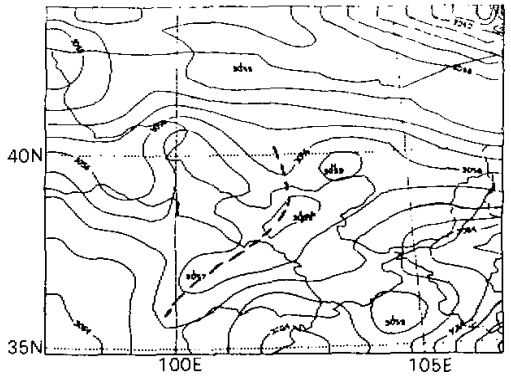

Fig.3. Field of the geopotential height at 700 hPa on 5 May 1993 at 1400 BJT.

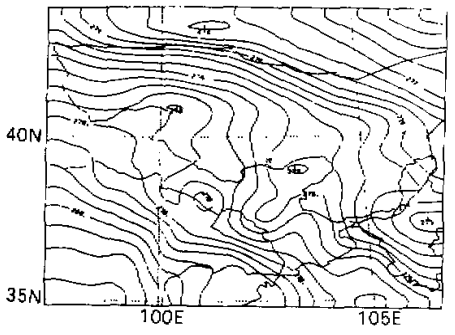

Fig.4. The temperature field of 700 hPa on 5 May 1993 at 1400 BJT.

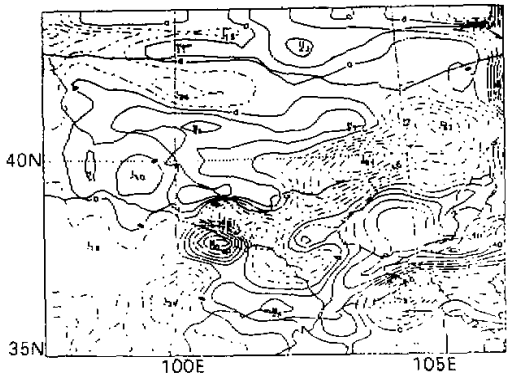

Fig.5. The vertical velocity distribution of 700 hPa on 5 May 1993 at 1700 BJT on the nest-grid map.

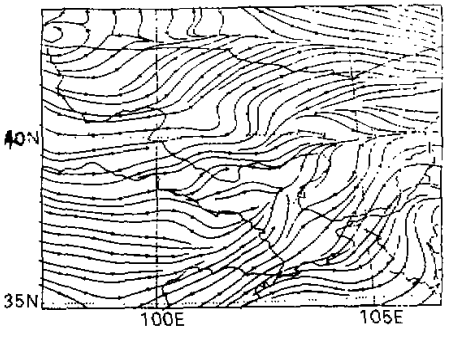

Fig. 6. The horizottal flow of 700 hPa on 5 May 1993 at 1700 BJT on the nest-grid map.

visibility occurred at that time. At 1630 BJT the center of the duststorm moved to Wuwei (37°N, 103°E); the moving speed of the cold front southeastward in 3 hr was about 300 km and the average wind velocity was 14 m / s. The simulated results basically agree to the observations.

3.1.2 *Distribution of dust concentrations*

As the sources of the dust were designated in Zhungeer Basin and Hexi Corridor, and the friction velocity is 50 cm / s, the distribution of the dust concentrations in the lowest level of the model, after integrating 33 hrs, yielded a result as shown in Fig. 7 (concentration unit in natural logarithm). At 1700 BJT the dust storm arrived at the center of Gansu province, including Jinchang City, where the dust concentrations in the surface layer would

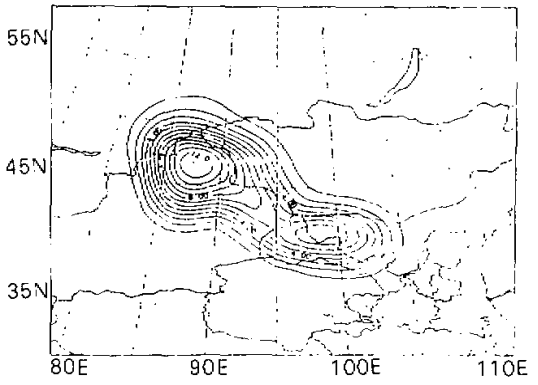

Fig. 7. The horizontal concentration distribution of the super duststorm in the surface layer on 5 May 1993 at 1700 BJT (u_* = 50 cm / s, line intervals in $\ln C(r)$, unit = number / m^3).

be 10^6—10^8 / m^3 (for an average dust particle radius of 10 μm). The field measurement of 10^8 / m^3 was in close agreement with the model result.

Figure 8a depicts the dust particle size at various height in the center of the duststorm. Near the surface layer, concentrations of dust particles of all size were high. As the altitudes increased, the concentration of the large particles decreases rapidly, while the distribution of dust concentrations of small particles decreases slowly. Fig 8b demonstrates the distribution of dust concentrations of varying dust size in the center of the duststorm. All dust concentrations decrease with height, but the rate of decrease is greater for larger particles than for small ones. During the duststorm transport process the larger particles will be deposited by the effect of gravity, and the smaller particles will be entrained into higher levels. A dustwall containing high concentrations of particles in a wide-range of size was observed below 400 m on 5 May. The model result in Fig 8b agrees with the observation.

3.2 *Cass B*

The simulated conditions were the same as case A, but the effect of the dust particles on radiation was added. For 5 May at 0800 and 1400 BJT, the temperature variations with height in the duststorm area are shown in Figs. 9a and 9b. At 0800 BJT before the duststorm arrived, the temperature profile had no obvious characteristics. At 1400 BJT as the dustwall passed through the location, the heating effect in the lower level was diminished to zero by the dust, and maximum heating occurs at the top of model. After the cold front passed through location, in 3 hr the temperature decreased as much as 18.4°C. The simulated results were indeed close to the field observation, which had registered 18°C cooling in Jinchang City.

The pressure and temperature fields of 750 hPa isobaric surface on 5 May at 1400 BJT indicated that the cold trough is deepening in the duststorm area. The rate of the cooling by the dust on 700 hPa was 1.5—2.0°C / hr, and on 500 hPa was 0.5—1.5°C / hr.

At 1700 BJT when the duststorm arrived at central Gansu province, the dust impact extended to the central Hexi Corridor, causing steeper temperature and pressure gradients. On 700 hPa the rate of cooling due to the airborne dust was 1.5°C / hr, and on 500 hPa was 1°C / hr.

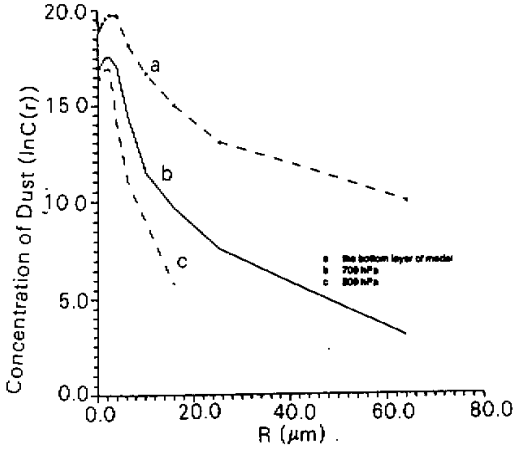

Fig. 8(a). The concentration spectrum (LnC(r)) versus dust radius at various heights on 5 May 1993 at 1700 BJT.

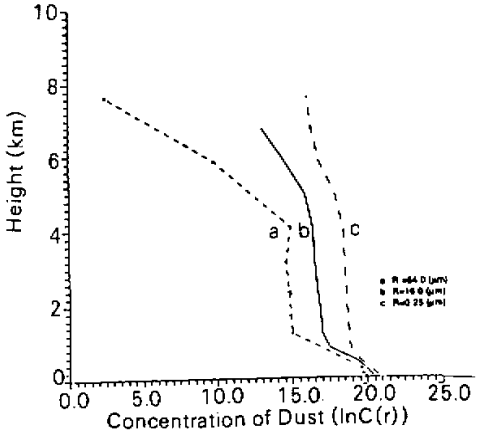

Fig. 8(b). The concentration at various heights for different size dust particles on 5 May 1993 at 1700 BJT.

In conclusion, the model results show that in the presence of dust plume, the solar shortwave radiation will be reduced because of the scattering effects of the dust particles, which induce general cooling in the lower troposphere at daytime.

IV. CONCLUSION

1) On 4–7 May 1993, a strong clod wind storm passed through the northwestern China, and a typical mesoscale system was developed, which generated a super duststorm in many provinces. The narrow Hexi topographic effect contributed greatly to the strong flow and

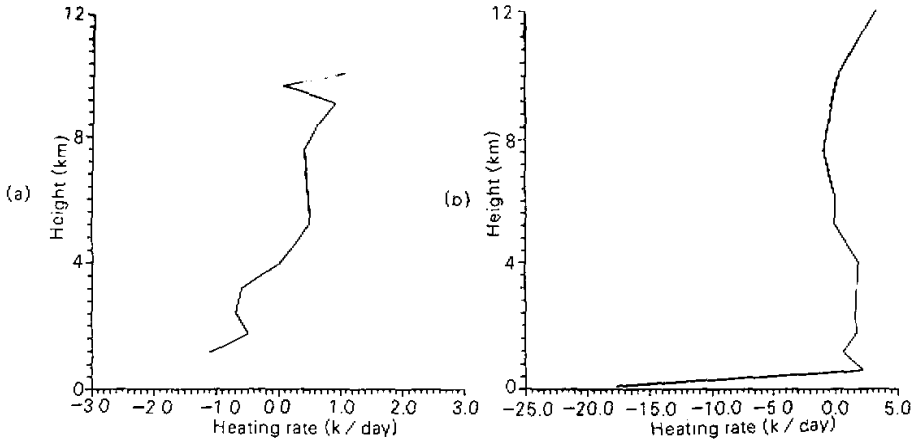

Fig.9 Vertical variation of the heating rate in the duststorm area on 5 May (a) at 0800 BJT; (b) at 1400 BJT.

duststorm transport. The entire dynamic and thermal conditions were playing an important role for the super duststorm.

2) In the center of the duststorm, the concentrations of the various particle sizes decrease with height, but the concentration decreased with height for small sizes is much slow than that of larger particles. During the duststorm transport process the large particles deposit by gravity effect, and the smaller particles will be entrained into higher levels. A dustwall is occurred below 400 m height by simulated results.

3) As the dustwall passed through the location, the heating effect in the lower level was diminished to zero by the dust, the temperature decreased in 3 hr as much as 18.4°C by simulated, which closed to 18°C by observed.

4) The duststorm arrived to central Gansu province, causing steeper temperature and pressure gradients, on 700 hPa the ratio of the decreasing temperature by the dust is 1.5°C / hr, and on 500 hPa is about 1.0°C / hr.

REFERENCES

Anthes, R. A, and T. T. Warner (1978), Development of hydrodynamic models suitable for air pollution and other mesometeorological studies, *Mon, Wea. Rev.*, **106**: 1045–1078.

Berkofski, L. (1982), A heuristic investigation to evaluate the feasibility of developing a desert dust prediction model. *Mon. Wes. Rev.*, **110**: 2055–2062.

Gillette, D. A. et al. (1981) Threshold velocities for input of soil particles into the air by desert soil. *J. G. R.*, **85**: 5621–5630.

Lee (1983), Simulation for transport and removal provesses of the Saharan dust, *J. Clim. Appl. Meteor.*, **22**: 623–629.

Schutz, L. (1980) Long-range transport of desert dust with special emphasis on the Saharan, *Ann. N. Y. Acad. Sci.*, **338**: 515–532.

Westphal, D. L., O. B. Toon and T. N. Carlson (1987), A two-dimensional numerical investigation of the dynamics and microphysics of Saharan dust storms, *J. G. R.*, **92**: 3027–3049.